

Figure S1

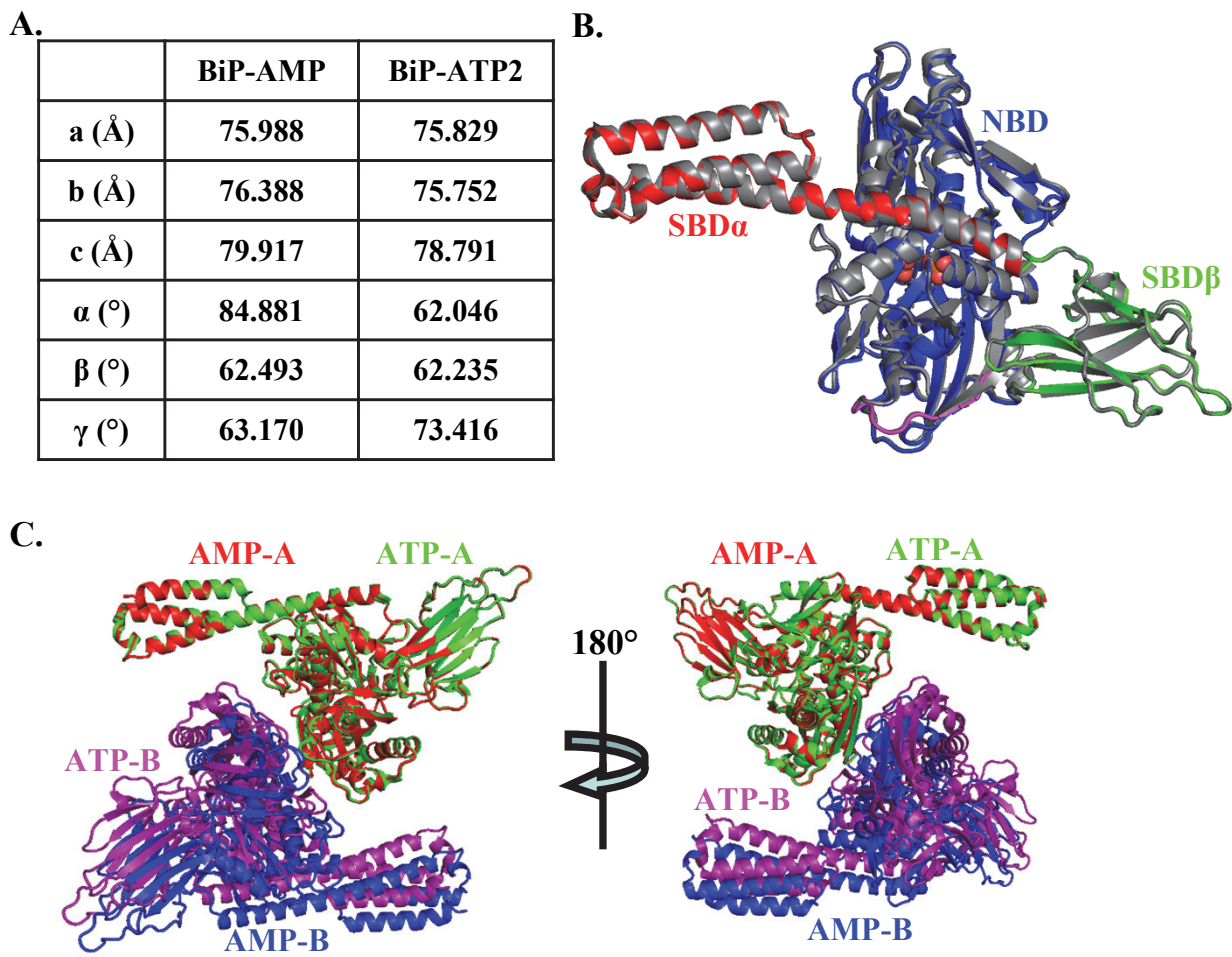


Figure S1 – Comparison of the BiP-AMP structure with the BiP-ATP2 structure.

A. The unit cell dimensions of the BiP-AMP and BiP-ATP2 (PDB: 6ASY) structures. The BiP-AMP structure was solved in this study with the crystals grown at pH 4.5. The space group for both structures is P1.

B. An orthogonal view of Fig. 1B.

C. The relative position of the two molecules of BiP in the asymmetric unit in the BiP-AMP and BiP-ATP structures. Protomer A was aligned. The colorings of the protomers are: red for the protomer A from the BiP-AMP structure (AMP-A); blue for the protomer B from the BiP-AMP structure (AMP-B); green for the protomer A from the BiP-ATP structure (ATP-A); and purple for the protomer B from the BiP-ATP structure (ATP-B).

Figure S2

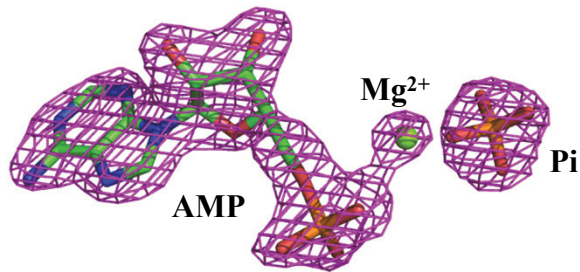


Figure S2 – The omit map for the AMP, Pi and associated Mg ion in the BiP-AMP structure.

The omit map was calculated and shown as purple mesh (contoured at 1.6 sigma). For the AMP and Pi, sticks were shown, and the bound Mg ion was represented as a green ball.

Figure S3

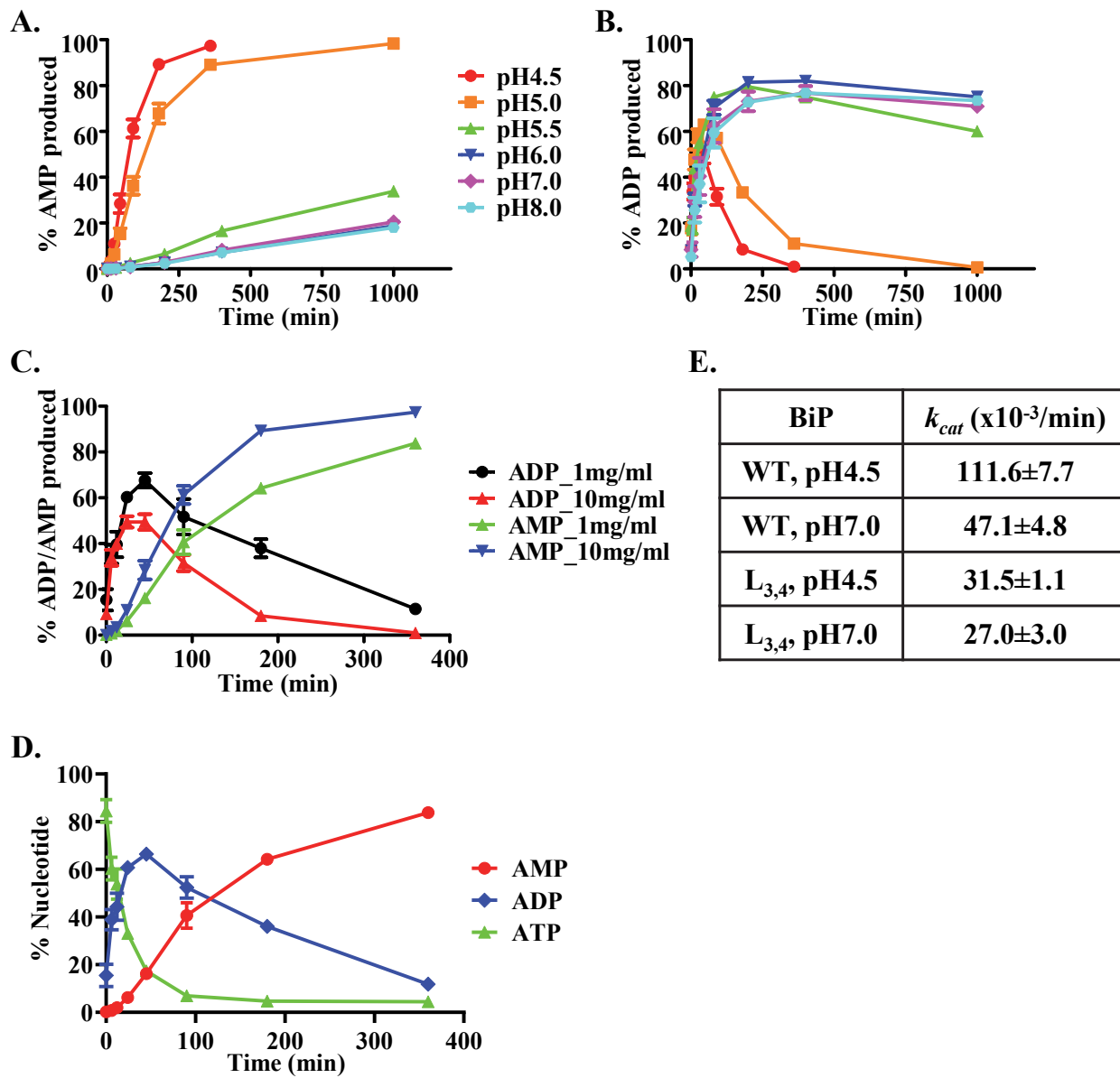


Figure S3 – The BiP proteins hydrolyze ATP to AMP at the acidic pH conditions.

A and **B**, The ATP hydrolysis to ADP (**A**) and AMP (**B**) by the BiP_L_{3,4} protein at different pH conditions. BiP protein was at 10 mg/ml, the crystallization protein concentration. The pH values were labeled on the right in **A**.

C, Comparison of the AMP and ADP hydrolysis by the BiP_L_{3,4} protein at 10 mg/ml and 1 mg/ml at pH 4.5.

D, The percentage of each nucleotide during the ATP hydrolysis by the BiP_L_{3,4} protein at pH 4.5 for 1 mg/ml. The data are the same as in Fig. 2A, D, E.

E, The catalytic constants (k_{cat}) of the overall ATP hydrolysis by the BiP proteins. The values were calculated using the same way as Fig. 2F.

All the data were Mean±SEM from at least three independent experiments using more than two different protein purifications.

Figure S4

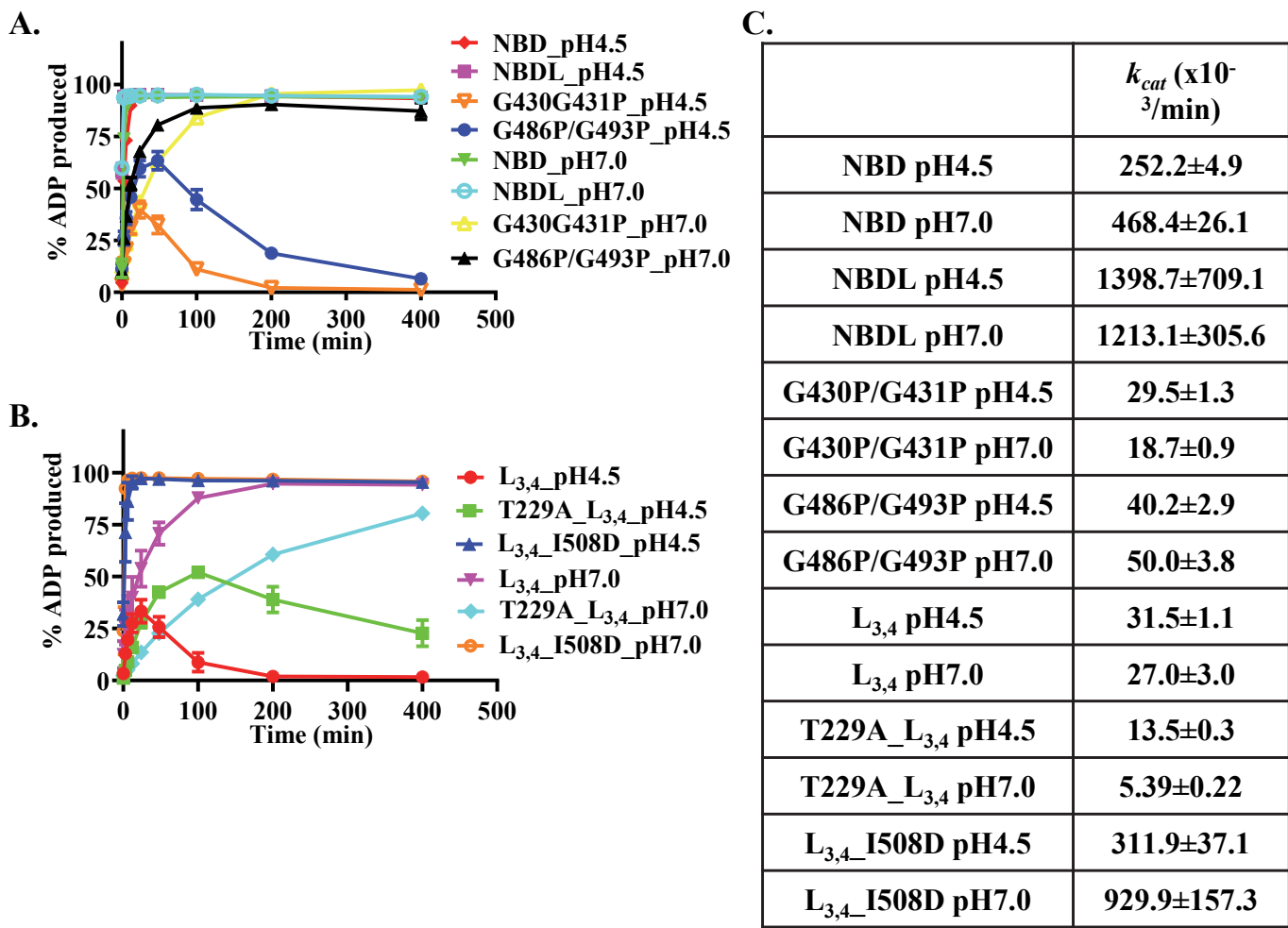


Figure S4 – The NBD-SBD contacts are crucial for the ATP to AMP hydrolysis

A, B, The ATP to ADP hydrolysis of the BiP mutations corresponding to the ATP to AMP hydrolysis in Fig. 4B and C.

C. The catalytic constants (k_{cat}) of the overall ATP hydrolysis for A, B, and Fig. 4B and C. The values were calculated the same way as Fig. 2F (Mean \pm SEM from three independent experiments using at least two different protein purifications).

Figure S5

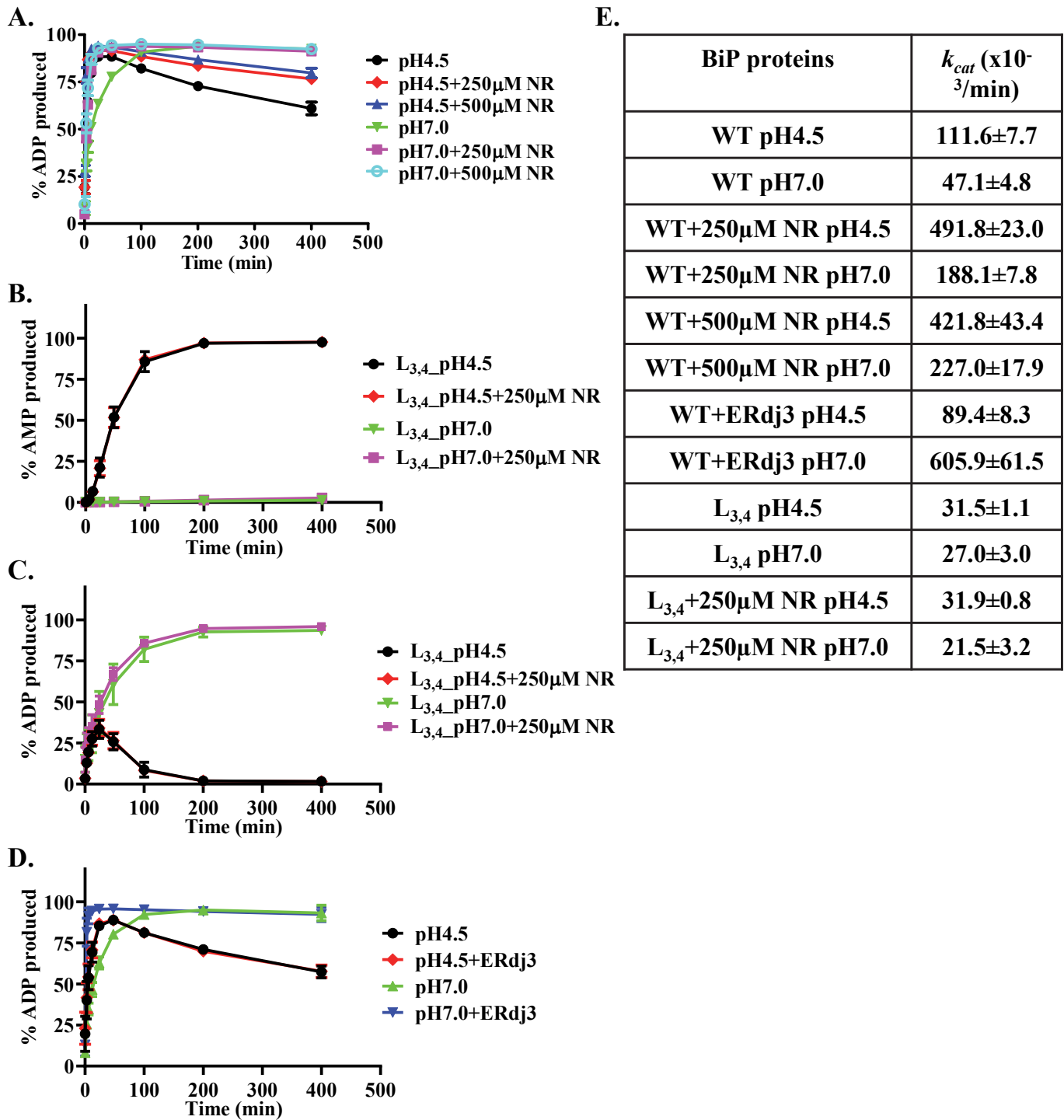


Figure S5 – Peptide substrate inhibits the ATP to AMP hydrolysis whereas ERdj3 has little effect on the ATP to AMP hydrolysis.

A, The ATP to ADP hydrolysis of WT BiP in the presence of the peptide substrate NR. The plots corresponded to the AMP hydrolysis in Fig. 5A.

B, and **C,** The ATP to AMP (**B**) and ATP to ADP (**C**) hydrolysis by the BiP-L_{3,4} protein were not appreciably affected by the NR peptide. The hydrolysis to AMP and ADP were from the same reactions in the presence or absence of the peptide substrate NR.

D, The ATP to ADP hydrolysis of WT BiP in the presence of ERdj3. The plots corresponded to the AMP hydrolysis in Fig. 5B.

E, The catalytic constants (k_{cat}) of the overall ATP hydrolysis for **A**, **B**, **C**, **D**, and Fig. 5A and **B**. The values were calculated using the same way as Fig. 2F (Mean±SEM from three independent experiments using more than two different protein purifications).

Figure S6

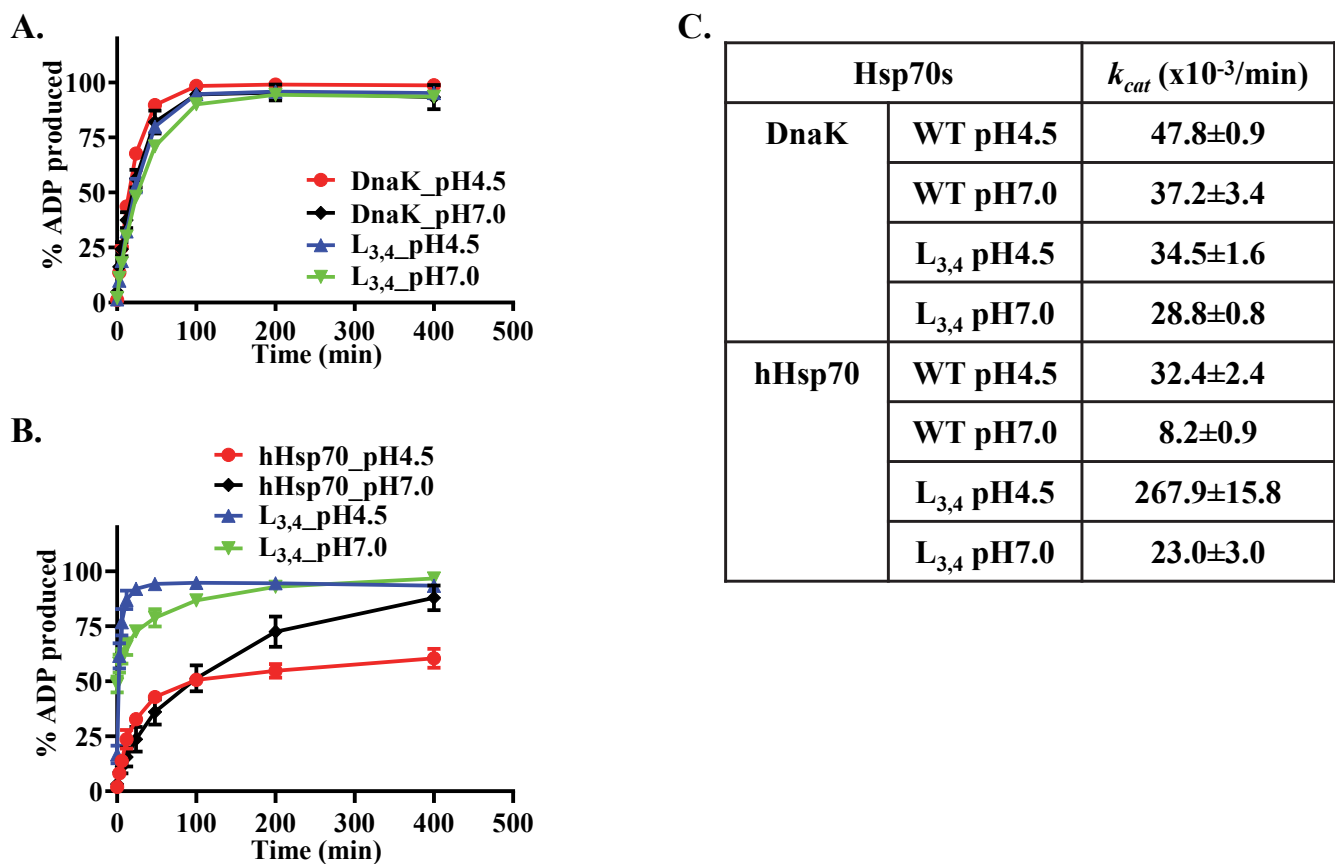
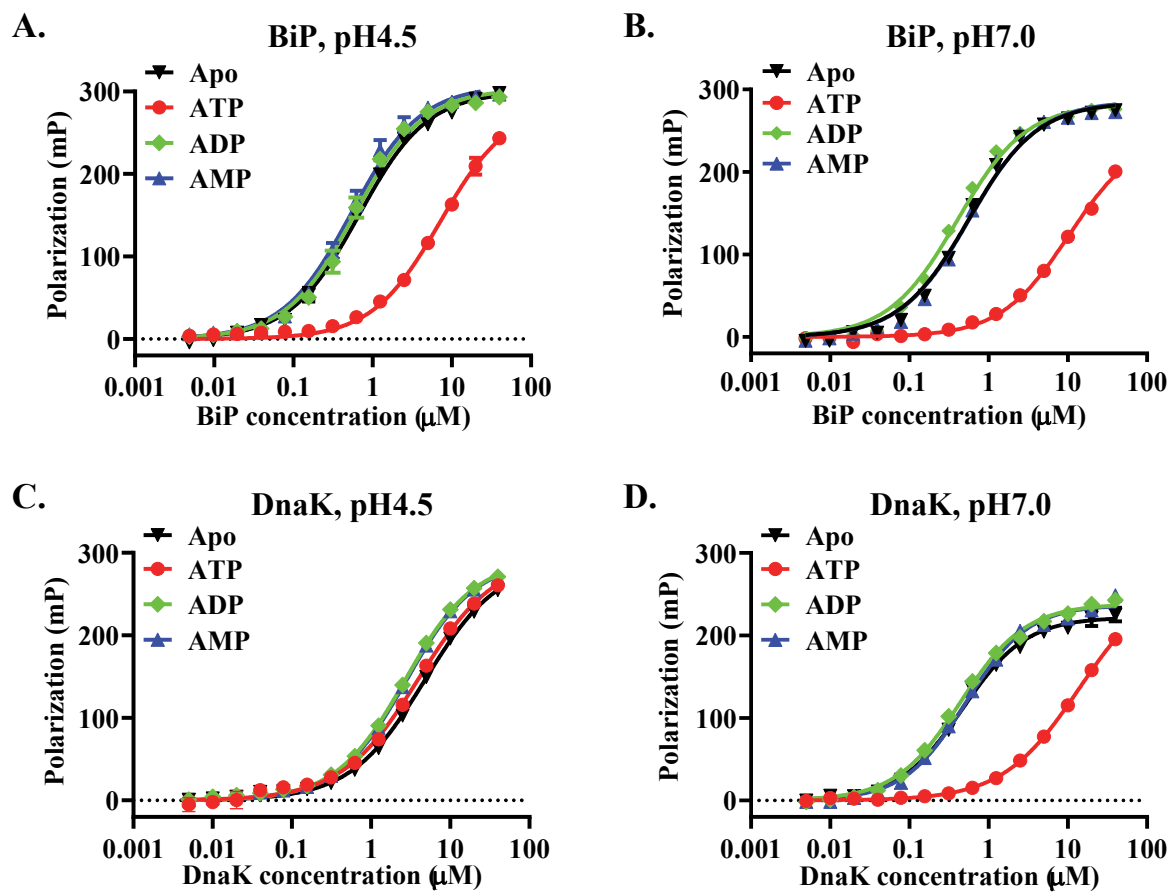


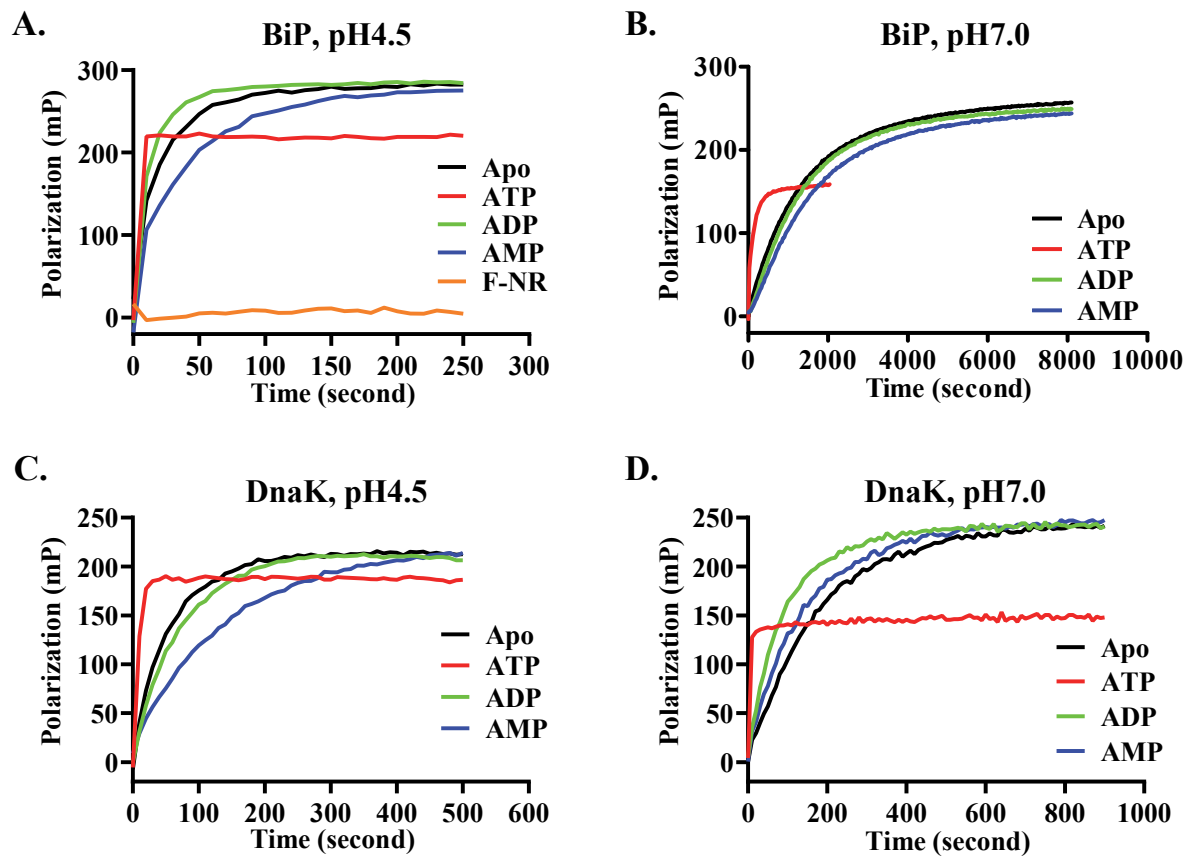
Figure S6 – The ATP to AMP hydrolysis is unique to BiP, not observed for either DnaK or human Hsp70.

A, B, The time courses of the ADP production by the DnaK proteins (**A**) and the hHsp70 proteins (**B**) corresponding to the ATP to AMP hydrolysis in Fig. 6A and **B**.

C, The catalytic constants (k_{cat}) of the overall ATP hydrolysis for **A, B**, Fig. 6A and **B**. The values were calculated using the same way as Fig. 2F (Mean±SEM from three independent experiments using more than two different protein purifications).

Figure S7**Figure S7 – The peptide substrate binding affinities.**

The binding affinity curves of the BiP (A and B) and DnaK (C and D) proteins for the NR peptide were measured at pH 4.5 (A and C) and 7.0 (B and D). The nucleotides were labeled. Apo: in the absence of nucleotide. Each data point was mean \pm SEM (from 2 independent experiments with 3 parallel measurements for each experiment).

Figure S8**Figure S8 – The peptide substrate binding kinetics.**

The binding kinetics of the BiP (A and B) and DnaK (C and D) proteins for the NR peptide were measured at pH 4.5 (A and C) and 7.0 (B and D). Proteins were at 20 μ M. The nucleotides were labeled. Apo: in the absence of nucleotide. Representative plots were shown.

Figure S9

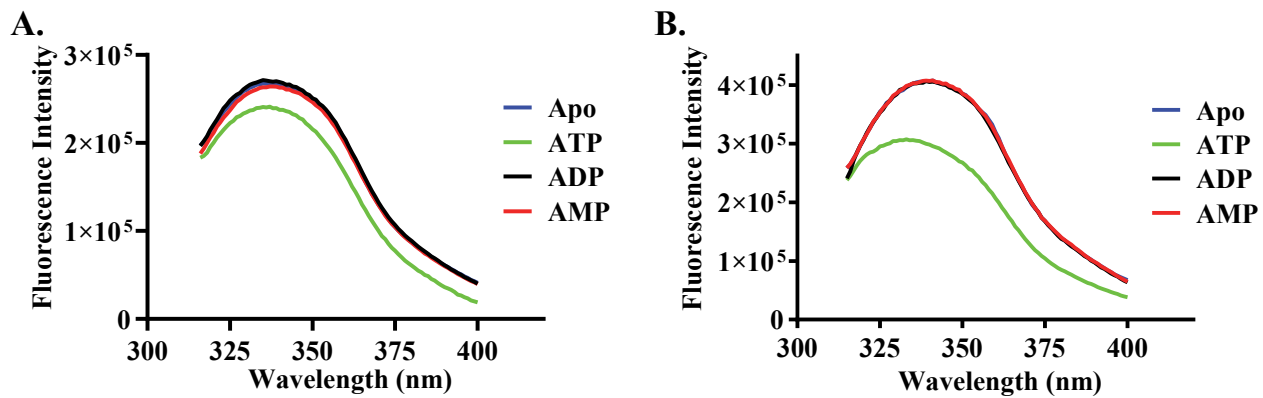


Figure S9 – The tryptophan fluorescence assay for nucleotide induced conformational changes in DnaK.

The DnaK protein (1 μ M) was incubated with different nucleotides for two minutes. Then fluorescence spectra were collected with excitation wavelength at 295 nm. The spectra in the absence of any nucleotide (Apo) were used as controls. **A**, pH 4.5; **B**, pH 7.5. Each spectrum is a representative of more than three independent experiments.

Figure S10

BiP	DnaK	hHsp70
D34	D8	D10
G36	G10	G12
T37	T11	T13
T38	T12	T14
Y39	N13	Y15
K96	K70	K71
E201	E171	E175
D224	D194	D199
G226	G196	G201
G227	G197	G202
G228	G198	G203
T229	T199	T204
G255	G229	G230
D259	D233	D231
E293	E267	E268
K295	K269	K270
R296	I270	R271
S298	S272	S273
G364	G341	G338
G365	G342	G339
S366	Q343	S340
R368	R345	R342
P390	P367	P365
D391	D368	D366

Figure S10 – The residues contacting ATP in Hsp70s.

The listed are the residues that contact ATP in the DnaK-ATP and BiP-ATP structures (pdb codes: 4JNE and 6ASY, respectively). Analogous residues in hHsp70 are based on sequencing alignment. The residues that are not identical among the Hsp70s are highlighted in red.